AMY

KEK Preprint 94-184
SAGA-HE-75
January 1995
H

A High-Q^2 Measurement of the Photon Structure Function F_2^γ

hep-ex 9510

AMY Collaboration

CERN LIBRARIES, GENEVA
SCAN-9503026

National Laboratory for High Energy Physics, 1995

KEK Reports are available from:

Technical Information & Library
National Laboratory for High Energy Physics
1-1 Oho, Tsukuba-shi
Ibaraki-ken, 305
JAPAN

Phone: 0298-64-1171
Telex: 3652-534 (Domestic)
(0)3652-534 (International)
Fax: 0298-64-4604
Cable: KEK OHO
E-mail: LIBRARY@JPNKEKVX (Bitnet Address)
library@kekvax.kek.jp (Internet Address)

A High-Q^2 Measurement of the Photon Structure Function F_2^γ

AMY Collaboration

S.K.Sahu [a], S.Ebara [b], T.Nozaki [c], S.Behari [a], H.Fujimoto [a], S.Kobayashi [a], A.Murakami [a], M.Yang [a], S.Matsumoto [b], K.Abe [c], Y.Fujii [c], Y.Kurihara [c], M.H.Lee [c], F.Liu [c], A.Maki [c], T.Omori [c], H.Sagawa [c], Y.Sakai [c], T.Sasaki [c], Y.Sugimoto [c], Y.Takaiwa [c], S.Terada [c], P.Kirk [d], T.J.Wang [e], A.Abashian [f], K.Gotow [f], M.E.Mattson [f], L.Piilonen [f], K.L.Sterner [f], S.K.Choi [g], C.Rosenfeld [h], L.Y.Zheng [h], R.E.Breedon [i], Winston Ko [i], R.L.Lander [i], J.Rowe [i], J.R.Smith [i], D.Stuart [i], S.Kanda [j], S.L.Olsen [j], K.Ueno [j], R.Tanaka [k], F.Kajino [l], T.Aso [m], K.Miyano [m], H.Miyata [m], N.Nakajima [m], K.Ohkubo [m], M.Oyoshi [m], M.Sato [m], M.Shirai [m], N.Takashimizu [m], Y.Yamashita [n], S.Schnetzer [o], J.Vinson [o], A.Bodek [p], B.J.Kim [p], C.Velissaris [p], J.S.Kang [q], D.Y.Kim [q], K.B.Lee [q], S.K.Kim [r], S.S.Myung [r], and D.Son [s]

[a] *Saga University, Saga 840, Japan*
[b] *Chuo University, Tokyo 112, Japan*
[c] *KEK, National Laboratory for High Energy Physics, Ibaraki 305, Japan*
[d] *Louisiana State University, Baton Rouge, LA 70803, USA*
[e] *Institute of High Energy Physics, Beijing 100039, China*
[f] *Virginia Polytechnic Institute and State University, Blacksburg, VA 24061, USA*
[g] *Gyeongsang National University, Chinju 660-701, South Korea*
[h] *University of South Carolina, Columbia, SC 29208, USA*
[i] *University of California, Davis, CA 95616, USA*
[j] *University of Hawaii, Honolulu, HI 96822, USA*
[k] *Japan Synchrotron Radiation Research Institute, Hyogo, 679-41, Japan*
[l] *Konan University, Kobe 658, Japan*
[m] *Niigata University, Niigata 950-21, Japan*
[n] *Nihon Dental College, Niigata 951, Japan*
[o] *Rutgers University, Piscataway, NJ 08854, USA*
[p] *University of Rochester, Rochester, NY 14627, USA*
[q] *Korea University, Seoul 136-701, South Korea*
[r] *Seoul National University, Seoul 151-742, South Korea*
[s] *Kyungpook National University, Taegu 702-701, South Korea*

Abstract

The photon structure function F_2^γ has been measured at average Q^2 values of 73 and 390 GeV^2 using data collected by the AMY detector at the TRISTAN e^+e^- collider. F_2^γ is observed to be increasing as $\ln Q^2$. The x-dependence of F_2^γ , where x is the momentum fraction carried by the parton inside the photon, is also measured. The measurements are compared with several parton density models.

1 Introduction

Because of the photon's point-like nature, the high Q^2 behaviour of its structure function, F_2^γ, can be calculated using perturbative QCD. This was first done by Witten and his leading order calculation suggested that F_2^γ measurements could provide the best method for measuring the QCD scale parameter Λ [1]. Subsequently, experimental measurements of the F_2^γ were made at PETRA and PEP [2, 3, 4, 5, 6]. However, the determination of Λ was not realized because the pointlike part of F_2^γ is badly singular in the small x region where higher order corrections were included [7, 8, 9]. Two methods were proposed to solve the problem. One is to calculate F_2^γ by solving the inhomogeneous Altarelli–Parisi (IAP) equations [10]. Another method, proposed by Field, Kapusta and Poggioli [11], is the introduction of a transverse-momentum cut-off, p_t^0, that defines the boundary of the phase space region where perturbative QCD is applicable. It was found that F_2^γ is, in fact, more sensitive to the choice of p_t^0 than to the value of Λ, and the determination of Λ from structure-function measurements is difficult. However, one can still test QCD by comparing the F_2^γ measurements with the QCD prediction by FKP. Such tests were done recently by the AMY [12], TOPAZ [13], and OPAL [14] groups.

The parton (quark and gluon) density in the photon is an essential ingredient in QCD calculations of jet production in quasi-real photon-photon collisions at e^+e^-

colliders [15, 16, 17, 18] as well as in photoproduction processes at ep colliders [19, 20]. Considering the significant role of these so-called resolved photon processes in the future high energy e^+e^- and $\gamma\gamma$ colliders [21], a knowledge of the photon's parton distribution becomes indispensable, which in turn, can be revealed by the measurement of the structure function F_2^γ.

Many theoretical attempts have been made recently to estimate the parton densities by solving the IAP equations. In these calculations the boundary conditions at low Q^2 are fixed either by fitting the evolved F_2^γ to its measured values or assuming some model. Since the statistical precision of existing F_2^γ determinations is still limited, additional measurements will help improve parton density determinations based on this technique. In turn, we can compare the presently available calculations of the parton density to the new, high-Q^2 measurements reported here.

High energy e^+e^-collisions are well suited for the study of collisions of quasi-real and virtual photons. Bremsstrahlung photons emitted from the beams have a considerable chance to collide with each other to produce hadrons via the process

$$e^+ + e^- \rightarrow e^+ + e^- + \textit{hadrons}, \qquad (1)$$

as illustrated in Fig. 1. Here q and k are the four-momenta of the two photons that collide to produce the hadronic system. In the special case when $k^2 \approx 0$ and $-q^2 \gg 0$, the electron associated with the q-photon gets scattered at a large angle, and is tagged in the detector, while the electron associated with the k-photon is scattered at a small angle close to the beam-line and escapes detection. Such a process can be described as the deep-inelastic electron-photon scattering, with the target photon being the k-photon.

In terms of laboratory variables, the cross section for this process is given by [22, 23]

$$\frac{d\sigma}{dE_{tag}d\cos\theta_{tag}} = \frac{4\pi\alpha^2 E_{tag}}{Q^4 y}\left[\left\{1+(1-y)^2\right\}F_2(x,Q^2) - y^2 F_L(x,Q^2)\right] \qquad (2)$$

where $Q^2 = -q^2 = 4E_{tag}E_{beam}\sin^2(\theta_{tag}/2)$, and θ_{tag} and E_{tag} are the scattering angle and energy of the tagged electron. The scaled variable $x = \frac{Q^2}{Q^2+W^2}$ represents the momentum fraction carried by the struck parton inside the photon, and $y = 1 - \frac{E_{tag}}{E_{beam}}\cos^2(\theta_{tag}/2)$. Here W is the invariant mass of the hadronic system.

The contribution from the F_L^γ structure function in Eq.(2) is estimated to be a few percent (several percent for our higher-Q^2 measurement) of the total for the kinematical conditions of the present experiment. Thus, measurements of the cross section of Eq.(2) provides a rather direct determination of F_2^γ.

We present here measurements of the photon structure function F_2^γ at average Q^2 values of 73 and 390 GeV^2, with a data sample that is an order-of-magnitude larger than that of our previous measurement [12]. We use these measurements to determine the value of the p_t^0 cut-off parameter at the average Q^2 of 73 GeV^2, and compare the results with those determined by the OPAL group at lower Q^2 values [14]. The results are also compared with several parametrizations of the parton density obtained from solutions of the IAP equations.

2 Experimental Apparatus and Event Selection

The data used are obtained with the AMY 1.5 detector of the TRISTAN e^+e^- collider at $\sqrt{s} = 58$ GeV[1], and correspond to an integrated luminosity of 309.8 pb^{-1}. Measurements of F_2^γ using the AMY 1.0 detector are reported in ref. [12];

[1]The endcap devices of the original AMY detector were upgraded in 1989. The original and upgraded detectors are referred to as AMY 1.0 and AMY 1.5, respectively.

a detailed description of the AMY detector is given in ref. [24]. We briefly note here features of the detector that are important for this analysis.

Charged particles are detected in a cylindrical drift chamber (CDC) with acceptance for $|\cos\theta| < 0.906$ and momentum resolution $\Delta p_t/p_t^2 \simeq 0.6\%$ GeV^{-1}. A cylindrical, lead/proportional-tube barrel electromagnetic shower counter (SHC) surrounds the CDC and has a total thickness of 14.5 radiation lengths. It has an acceptance of $|\cos\theta| < 0.75$ and an energy resolution of $\Delta E/E = 23/\sqrt{E(\mathrm{GeV})}+6\%$. The Endcap Shower Counter (ESC) consists of a 4.5 r.l.-thick "front" and an 8.9 r.l.-thick "back" lead/scintillator calorimeters with a resistive tube chamber between them for position measurement. The ESC covers the region $11^o < \theta < 37^o$ and has an energy resolution of $\Delta E/E = 15/\sqrt{E(\mathrm{GeV})} + 6\%$. Both the SHC and ESC are used to tag the scattered electrons.

SHC-tag events are selected as follows:

1. A charged particle track is identified as the tagged electron if it has an azimuthal angle $\theta \geq 43^0$ and is associated with an SHC cluster with an energy greater than $0.25E_{beam}$.

2. No additional SHC or ESC clusters with energy above $0.25E_{beam}$ are observed (anti-tagging cut).

3. At least five charged tracks are observed in the CDC.

4. The total visible energy is less than E_{beam}.

5. The invariant mass of the observed hadronic system $W_{vis} > 3$ GeV.

6. The projection of the sum of the transverse momenta of all particles in the same hemisphere as the tagged electron onto the direction of the tagged electron, $\Sigma p_{T,\parallel}$, is less than 1.5 GeV. (This ensures that the tagged electron is isolated from the hadron system.)

7. The Normalized Longitudinal Momentum Imbalance, NLMB, is greater than $0.15 + 0.075(\Sigma p_{T,\parallel})$, where NLMB$=\Sigma p_L/E_{beam}$ along the tag direction, and the sum runs over all charged and neutral particles, including the tagged electron.

A total of 77 events pass the above-mentioned cuts. We calculate backgrounds using Monte Carlo generators and a full detector simulation. The most serious background, from inelastic Compton scattering [25], is 30.5 ± 1.4 events. The background from $e^+e^- \to e^+e^-\tau^+\tau^-$ is 2.7 ± 0.2 events. Backgrounds from single-photon annihilation and beam–gas interaction events are negligibly small. After correcting for all these backgrounds, 43.8 ± 9.0 events remain, with an average Q^2 of 390 GeV^2. The trigger efficiency, determined from redundant independent triggers, is very near 100%.

The ESC tag events are selected using the following criteria :

1. A tagged electron is identified with a cluster that is observed between $15^\circ < \theta < 35^\circ$ in the ESC with energy greater than $0.5E_{beam}$.

2. No additional clusters with energy greater than $0.25E_{beam}$ are observed elsewhere in the detector (anti-tagging cut).

3. At least three charged particles are seen in the CDC, at least two of which must have $p_T \geq 750$ MeV.

4. The total visible energy is less than $0.4E_{beam}$.

5. NLMB is greater than 0.6 .

6. The Normalized Transverse Momentum Imbalance, NTMB is less than 0.2, where NTMB $= \frac{|\Sigma \vec{p_T}|}{E_{beam}}$ and the summation includes the tag electron.

A total of 610 events pass these cuts. Backgrounds from various sources are estimated as follows:

- 40.7 ± 5.9 events from the single-γ annihilation hadronic process;
- 36.4 ± 5.6 events from the $e^+e^- \to e^+e^-\tau^+\tau^-$ process;
- 18.6 ± 4.0 events from the inelastic Compton scattering process.

Backgrounds from $e^+e^- \to \tau^+\tau^-$, conversion and annihilation diagrams for $e^+e^- \to e^+e^-q\bar{q}$, and beam–gas interaction are negligibly small.

After the background subtraction, 514.3 ± 26.3 events remain. The trigger efficiency was determined from redundant, independent triggers to be 89.8%. The tagging efficiency was found to be 97%. The Q^2 values for these events range from 25 to 220 GeV^2, with an average Q^2 of 73 GeV^2.

3 Event Simulation

In order to compare experimental results with theoretical predictions, to make acceptance corrections for the unfolding procedure, and to decide on kinematical cuts, we generated a large Monte Carlo sample of events simulating process (1). The cross section for process (1) is given by convoluting the photon flux with the differential cross section given by Eq. (2) using the Equivalent Photon Approximation (EPA) [22, 26]. For the photon flux we use a formula that includes the effects of the anti-tagging condition [23]. Monte Carlo events were generated according to the FKP, QPM and VMD models. Contributions from the point-like part of F_2^γ to light-quark (u,d,s) production is simulated by means of the FKP formalism [11] and described in ref. [12], using $\Lambda = 0.2$ GeV for the QCD scale parameter and $p_t^0 = 0.5$ GeV as the cut-off defining the boundary between the point-like and hadron-like regimes of the photon. The heavy-quark (i.e., c and b) contribution to

the point-like part of F_2^γ is generated using the Quark Parton Model (QPM) [26]; QCD corrections for the heavy quarks are considered to be negligible. Since we also present our structure function with heavy quark contribution separated, this partition of FKP and QPM is convenient. For the hadronic part of the F_2^γ we used the Vector Meson Dominance (VMD) model parameterized as

$$F_2^{\gamma,VMD} = \alpha\left[0.22x^{0.31}(1-x)^{0.95} + 0.06(1-x)^{2.5}\right], \qquad (3)$$

by the TPC/2γ group [6].

For the longitudinal structure function F_L^γ we used the QPM prediction [25]. As mentioned above, the contribution of this part to the total cross section is estimated to be at the few percent (several percent) level for ESC- (SHC-) tag events, assuming the QPM prediction for both the F_2^γ and F_L^γ. For each process, we generated $e\gamma \to eq\bar{q}$ events according to the cross section formula given by Eq. (2) using the corresponding F_2^γ.

The angular distributions of the quark pairs for the point-like and the hadronic contributions are different. For the point-like contribution, we used the quark angular distribution given in ref. [22]. For the hadronic part, we used a transverse momentum distribution of the form $\frac{d\sigma}{dp_T^2} \propto e^{-\beta p_T^2}$, where p_T represents the transverse momentum of the quark with respect to the incident photon direction. We use β=3. For quark masses we use: $m_u = m_d = 325$ MeV; $m_s = 500$ MeV; $m_c = 1.6$ GeV; and $m_b = 5$ GeV.

The Monte Carlo integration and event generation are done with the BASES and SPRING programs [27]; and the LUND 6.3 string-fragmentation model [28] is used to simulate the final hadronic state out of the produced quarks. The generated events are passed through the AMY detector simulation program and analysed with the same programs that are used for the real data.

There are two assumptions implicit to our MC simulation. The first is that the

target photon mass is zero. Since our anti-tagging condition is rather loose, the actual target photon may have a finite virtual mass, while the photon structure function that we use is computed under the assumption of zero target photon mass. The second assumption is that initial-state radiative corrections are negligibly small. Neither assumption is strictly correct: radiative effects tend to increase the effective cross section, whereas massive photons reduce it. In order to estimate these effects, we compared a QPM event sample generated using our Monte Carlo with a sample produced by a generator developed by Berends, Daverveldt and Kleiss [31]. The latter is based on the exact calculation for all first order diagrams including radiative corrections to the multiperipheral diagram only. Since the multiperipheral diagram dominates the cross section, the comparison of the two MC results gives the necessary information.

For the ESC-tag events, the total cross sections within our acceptance cuts for the two MC event samples are same at one-percent level, which suggests that the effects of the finite target photon mass and radiative correction compensate each other as far as the total cross section is concerned. However, the Q^2 and the visible W (W_{vis}) distributions are slightly different, but different in such a way that the visible x (x_{vis}) distributions almost match each other. Therefore we do not make any corrections to the x_{vis} distribution while extracting F_2^γ.

For the SHC-tag events, the radiative correction increases the cross section by 6% and the target photon mass effect decreases the cross section by 10%; the combined effect decreases the cross section by 5 %. The effects on the Q^2, W_{vis} and x_{vis} distributions are similar to those for the ESC-tag case except for the absolute normalization. Thus, we reduce the total number of events calculated by our MC by 5% and apply no other corrections.

After applying the same cuts as those used for real data, the relative contributions from the different MC event types are in the ratio of

FKP : QPM : VMD = 56 : 23 : 21 at Q^2 = 73 GeV^2 and 51 : 38 : 11 at Q^2 = 390 GeV^2. The numbers of events expected from the Monte Carlo calculations are 487.9 ± 8.7 for the ESC- and 44.2 ± 0.8 for the SHC-tags, which agree with those from the real data, i.e. 514.3 ± 26.3 and 43.8 ± 9.0, respectively. Various distributions of kinematic parameters, such as NLMB, NTMB, W_{vis}, visible total energy, number of charged/neutral tracks, Q^2, polar angle/energy of the tagged electron, for the real data agree with those expected from the MC in both the tag cases. As an example, we show the x_{vis} distributions for the SHC- and ESC-tag events in Fig. 2.

4 Analysis and Result

In order to extract F_2^γ, we unfold the experimental data using a correlation matrix that includes the effects of the detector acceptance and resolution as determined from our Monte Carlo data sample. To extract the x dependence of F_2^γ, we use x_{vis} as the unfolding variable.

The ESC (SHC) data are unfolded in 8 x-bins and later combined to three (two) bins using the unfolding technique described in ref. [3]. The resulting F_2^γ values at different x-bins are presented in Table 1.

Tag Device	$< Q^2 >$	x	$< F_2^\gamma/\alpha >$
ESC tag	73 GeV^2	0.25	$0.65 \pm 0.08 \pm 0.06$
		0.50	$0.60 \pm 0.16 \pm 0.03$
		0.75	$0.65 \pm 0.11 \pm 0.08$
SHC tag	390 GeV^2	0.31	$0.94 \pm 0.23 \pm 0.10$
		0.69	$0.82 \pm 0.16 \pm 0.11$

Table 1. Unfolded F_2^γ measurements.

In Table 1, the first errors are statistical and the second are systematic. The systematic errors are the quadratic sum of the following:

- a 1.5% uncertainty in the measurement of luminosity;
- a 1% uncertainty in the ESC-tag trigger efficiency (0% for the SHC tag);
- an error ranging from 3 $\sim$ 5% due to the ESC-tag event selection cuts and background rejection (negligible for SHC-tags).
- a fragmentation function uncertainty error ranging from 2 $\sim$ 11 % for the ESC-tag and from 4 $\sim$ 11 % for SHC-tag events. This was estimated from the amount of variation of the unfolded F_2^γ using different fragmentation models : (a) LUND 6.3 fragmentation default parameters [28]; (b) same tuned for TRISTAN data [29]; and (c) independent fragmentation model [30].
- an error due to the assumption that F_2^γ can be factorized into x and Q^2 functions. This was estimated by unfolding QPM MC events with a correlation matrix computed for a sample generated with $F_2^\gamma = \alpha \ln Q^2$. Its bin-to-bin variation is 5 $\sim$ 6 % for the ESC-tag and 3 $\sim$ 11 % for the SHC-tag events.

The measured F_2^γ functions are shown in Figs. 3(a) and 3(b), where the error bars indicate the quadratic sum of the statistical and systematic uncertainties. Included in the figure are the theoretical predictions based on the FKP model for F_2^γ at $Q^2 = 73$ GeV^2 and $Q^2 = 390$ GeV^2 for various values of p_t^0. These are calculated by summing the QCD prediction in all orders for the light quarks (u,d,s) with $\Lambda = 0.2$ GeV, the QPM prediction for the heavy quarks (c and b), and the VMD contribution for the hadronic part.[2] As seen in the figure, the data are consistent with the predictions for p_t^0 values below 1 GeV. The best value of p_t^0 for the ESC-tag data, determined by fitting the data in the range $25 < Q^2 < 175$ GeV^2

[2]In the prediction for the QPM part, we have assumed the charm quark mass to be 1.6 GeV. A lower charm mass (1.3 GeV, for example) increases the F_2^γ at higher x, as shown in Figs. 3(e) and 3(f). In calculating the average F_2^γ such an ambiguity enters as a systematic error.

to the FKP predictions, is $p_t^0 = 0.51 \pm 0.39$ GeV, with $\chi^2/DOF = 0.53/2$. This value is larger than, but consistent with, the p_t^0 value obtained by the OPAL group [14], namely 0.27 ± 0.10 GeV for the range $4 < Q^2 < 40$ GeV^2.

As mentioned above, various theoretical predictions of F_2^γ are available, all of which are obtained by solving either the leading-order (LO) or the higher-order (HO) IAP equations. They differ from each other by the methods used to determine the parton distributions at Q_0^2, the lower boundary of Q^2. Most of them determine the parton density at the boundary around 4 GeV^2 by fitting the evolved F_2^γ function to the measured F_2^γ data. Among the predictions of this type are those by Drees-Grassie (DG) [32], Levy-Abramowicz-Charchula (LAC) [33] and Watanabe-Hagiwara-Izubuchi-Tanaka (WHIT) [34]. The predictions by Glück-Reya-Vogt (GRV) [35] and Aurenche-Fontannaz-Guillet (AFG) [36] use VMD and modified-VMD predictions, respectively, for the boundary condition at the rather low Q_0^2 value of 0.3 GeV^2. The DG, LAC and WHIT predictions are leading-order calculations while the GRV and AFG predictions include both the leading- and higher-order contributions. When both the LO and HO predictions are available, we show here only the HO predictions although the difference of the two predictions is very small. The parton densities for DG, LAC and GRV were calculated using the PDFLIB program [37], but parton densities for WHIT and AFG were calculated by the programs supplied by the respective authors.

The WHIT and AFG predictions explicitly take into account the heavy quark mass effects, but the other calculations neglect them [38]. Thus, the F_2^γ predictions of the DG,LAC and GRV models are taken to be the sum of the QCD prediction for the light quarks and the QPM prediction for the heavy quarks, while the WHIT and AFG models give QCD predictions for F_2^γ for all flavours.

In Figs. 3(c) and 3(d) we compare the F_2^γ measurements with the DG, LAC1[3]

[3]Out of the three LAC models LAC1, LAC2 and LAC3, the last one has already been

and WHIT[4] predictions. These predictions are in good agreement with the data. Figs. 3(e) and 3(f) show comparisons with the GRV and AFG predictions. They also exhibit good agreement with our data.

The values of F_2^γ averaged over the x-range $0.3 < x < 0.8$ are :

- $F_2^\gamma = 0.63 \pm 0.07$ at $Q^2 = 73$ GeV^2;
- $F_2^\gamma = 0.85 \pm 0.18$ at $Q^2 = 390$ GeV^2.

The listed uncertainties are the quadrature sum of the statistical and systematic errors. The values of F_2^γ with the heavy quark (c,b) contribution subtracted are $F_2^\gamma = 0.42 \pm 0.08$ (0.50 ± 0.18) for the ESC- (SHC-) tag data. Here the errors include the effect of the c-quark mass uncertainty, estimated by allowing it to vary between 1.3 and 1.6 GeV (see Figs. 3(e) and 3(f)). According to QCD, F_2^γ should increase as $\ln Q^2$. In Fig. 4 we plot the values of F_2^γ with the heavy quarks removed together with the corresponding values from the other experiments [13, 14, 23]. Included in the figure are the FKP predictions for various p_t^0 values. The data are consistent with a $\ln Q^2$ increase. Fitting the FKP prediction to all the data gives a p_t^0 value of 0.45 ± 0.07 GeV with $\chi^2/DOF = 4.36/13$.

5 Summary

In summary, we have measured the photon structure function F_2^γ at high Q^2. The measurements are compared with various QCD-based predictions. The x behaviour of F_2^γ at $Q^2 = 73$ GeV^2 and $Q^2 = 390$ GeV^2 are consistent with the FKP, WHIT, AFG, DG, LAC1 and GRV predictions. The measured Q^2 behaviour of F_2^γ is consistent with the $\ln Q^2$ increase, as predicted by QCD. By fitting the

experimentally rejected [15]. LAC1 and LAC2 give similar F_2^γ functions. Therefore we chose to compare our data with LAC1 only.

[4]There are six versions of the WHIT model, but all of them have similar F_2^γ functions, except at very low x. Hence we show only the WHIT1 result.

FKP prediction to our data alone and to all the available F_2^γ data, we obtain p_t^0 values of 0.51 ± 0.39 and 0.45 ± 0.07 GeV, respectively.

6 Acknowledgement

We thank the TRISTAN staff for the excellent operation of the storage ring. We acknowledge the strong support provided by the staffs of our home institutions. We would like to thank K. Hagiwara and M. Fontannaz for providing us with their programs that calculate the WHIT and AFG parton densities, respectively. This work has been supported by the Japan Ministry of Education, Science and Culture (Monbusho), the Japan Society for the Promotion of Science, the US Department of Energy, the US National Science Foundation, the Korean Science and Engineering Foundation, the Ministry of Education of Korea, and the Academia Sinica of the People's Republic of China.

References

[1] E. Witten, Nucl. Phys. **B120** (1977) 189.

[2] PLUTO Collab., Ch. Berger et al., Z. Phys. **C26** (1984) 353; Phys. Lett. **B142** (1984) 111; Phys. Lett. **B149** (1984) 421; Nucl. Phys. **B281** (1987)365.

[3] JADE Collab., W. Bartel et al., Z. Phys. **C24** (1984) 231.

[4] TASSO Collab., M. Althoff et al., Z. Phys. **C31** (1986) 527.

[5] CELLO Collab., H.J. Behrend et al., Phys. Lett. **B126** (1983) 391.

[6] TPC/2γ Collab., H. Aihara et al., Z. Phys. **C34** (1987) 1; Phys. Rev. Lett. **58** (1987) 97; D. Bintinger et al., Phys. Rev. Lett. **54** (1985) 763.

[7] W.A. Bardeen and A.J. Buras, Phys. Rev. **D20** (1979) 166;**D21** (1980) 2041(E).

[8] D.W. Duke and J.F. Owens, Phys. Rev. **D22** (1980) 2280.

[9] G. Rossi, Phys. Lett. **B130** (1983) 105; Phys. Rev. **D29** (1984) 852.

[10] M. Glück and E. Reya, Phys. Rev. **D28** (1983) 2749; M. Glück, K. Grassi, and E. Reya; Phys. Rev. **D30** (1984) 1447.

[11] J.H. Field, F. Kapusta, and L. Poggioli, Phys. Lett. **B181** (1986) 362; Z. Phys. **C36** (1987) 121; F. Kapusta, Z. Phys. **C42** (1989) 225.

[12] AMY Collab., T. Sasaki et al., Phys. Lett. **B252** (1990) 491.

[13] TOPAZ Collab., K. Muramatsu et. al., Phys. Lett. **B332** (1994) 478.

[14] OPAL Collab., R. Akers et al., Z. Phys. **C61** (1994) 199.

[15] AMY Collab., R. Tanaka et. al., Phys. Lett. **B277** (1992) 215.

[16] AMY Collab., B.J. Kim et. al., Phys. Lett. **B325** (1994) 248.

[17] TOPAZ Collab., H. Hayashii et. al., Phys. Lett. **B314** (1993) 149.

[18] ALEPH Collab., D. Buskulic et. al., Phys. Lett. **B313** (1993) 509.

[19] H1 Collab., T. Ahmed et. al., Phys. Lett. **B297** (1992) 205.

[20] ZEUS Collab., M. Derrick et. al., Phys. Lett. **B297** (1992) 404.

[21] M. Drees and R. Godbole, Phys. Rev. Lett. **67** (1991) 1189.

[22] S.J. Brodsky, T. Kinoshita and H. Terazawa, Phys. Rev. Lett. **27** (1971) 280; Phys. Rev. **D4** (1971) 1532.

[23] Ch. Berger and W. Wagner, Phys. Rep. **146** (1987) 1.

[24] AMY Collab., T. Kumita et al. Phys. Rev. **D42** (1990) 1339.

[25] C. Peterson et al., Nucl. Phys. **B174** (1980) 424.

[26] V.M. Budnev et al., Phys. Rep. **15** (1975) 181.

[27] S. Kawabata, Comp. Phys. Comm. **41** (1986) 127.

[28] T. Sjöstrand, Comp. Phys. Comm. **39** (1986) 347; T. Sjöstrand and M. Bengtsson, Comp. Phys. Comm. **43** (1987) 367.

[29] AMY Collab., Y.K.Li et al., Phys. Rev. **D41** (1990) 2675.

[30] R.D. Field and R.P.Feynman, Nucl. Phys. **B136** (1978) 1.

[31] F.A. Berends, P.H. Daverveldt and R. Kleiss, Comp. Phys. Comm. 40 (1986) 271; Nucl. Phys. **B253** (1985) 441.

[32] M. Drees and K. Grassie, Z. Phys. **C28** (1985) 451.

[33] H. Abramowitz, K. Charchula and A. Levy, Phys. Lett. **B269** (1991) 458.

[34] K. Hagiwara, M. Tanaka, I. Watanabe and T. Izubuchi, KEK Preprint 93-160.

[35] M. Glück, E. Reya and A. Vogt, Phys. Rev. **D46** (1993) 1973.

[36] P. Aurenche, J.-Ph. Guillet and M. Fontannaz, LPTHE Orsay 93-37.

[37] H. Plothow–Besch, CERN-PPE/92-123.

[38] In the GRV paper the heavy quark mass effects are taken into account [35], but the PDFLIB formula for GRV neglects them [37].

Figure Captions

Fig. 1 : Deep-inelastic electron-photon scattering in e^+e^- collisions.

Fig. 2 : The x_{vis} distributions for the **(a)** ESC-tag and **(b)** SHC-tag events. The data (crosses) corrected for the background contributions bin by bin are compared with the FKP(uds)+QPM(cb)+VMD prediction (histogram) for p_t^0 = 0.5 GeV, Λ = 0.2 GeV, m_c = 1.6 GeV and m_b = 5.0 GeV.

Fig. 3 : The F_2^γ values as a function of x.

(a) ESC-tag and **(b)** SHC-tag events. The data (closed circles) are compared with the FKP(uds)+QPM(cb)+VMD predictions with p_t^0=0.1 (solid), 0.5 (dashed) and 1.0 GeV (dotted) for Λ = 0.2 GeV, m_c = 1.6 GeV and m_b = 5.0 GeV. The QPM(c,b) (dot-dashed) and VMD (double-dot-dashed) contributions are shown separately .

(c) ESC-tag and **(d)** SHC-tag events. The data (closed circles) are compared with the WHIT1(solid), LAC1 (dashed) and DG (dot-dashed) model predictions. The heavy quark contribution for the WHIT1 (double-dot-dashed) is shown separately. The heavy quark contribution for the DG and LAC calculated by QPM is shown in Figs. 3(a) and 3(b).

(e) ESC-tag and **(f)** SHC-tag events. The data (closed circles) are compared with the GRV (solid) and AFG (dashed) model predictions. The QPM c-quark contribution is shown for c-quark masses of 1.3 and 1.6 GeV.

Fig. 4 : The Q^2–evolution of the structure function F_2^γ for the x-region between 0.3 and 0.8. The c- and b-quark contributions are subtracted. Our measurements are shown together with those from other experiments. Included in the figure are the FKP(uds)+VMD predictions for p_t^0=0.1 (dotted), 0.5 (solid) and 1.0 GeV (dashed). The VMD contribution(dot-dashed) is indicated separately.

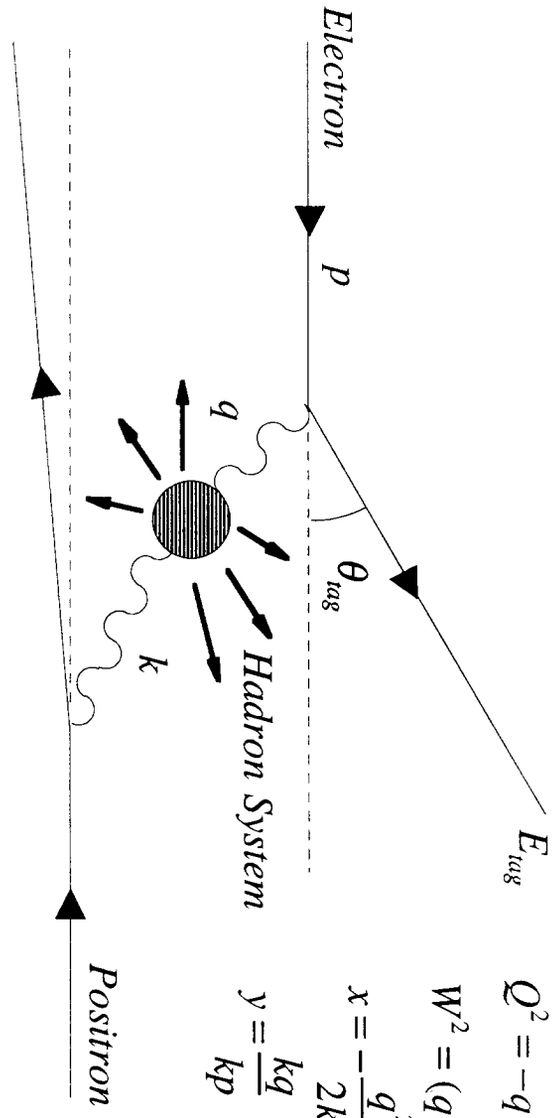

Figure 1

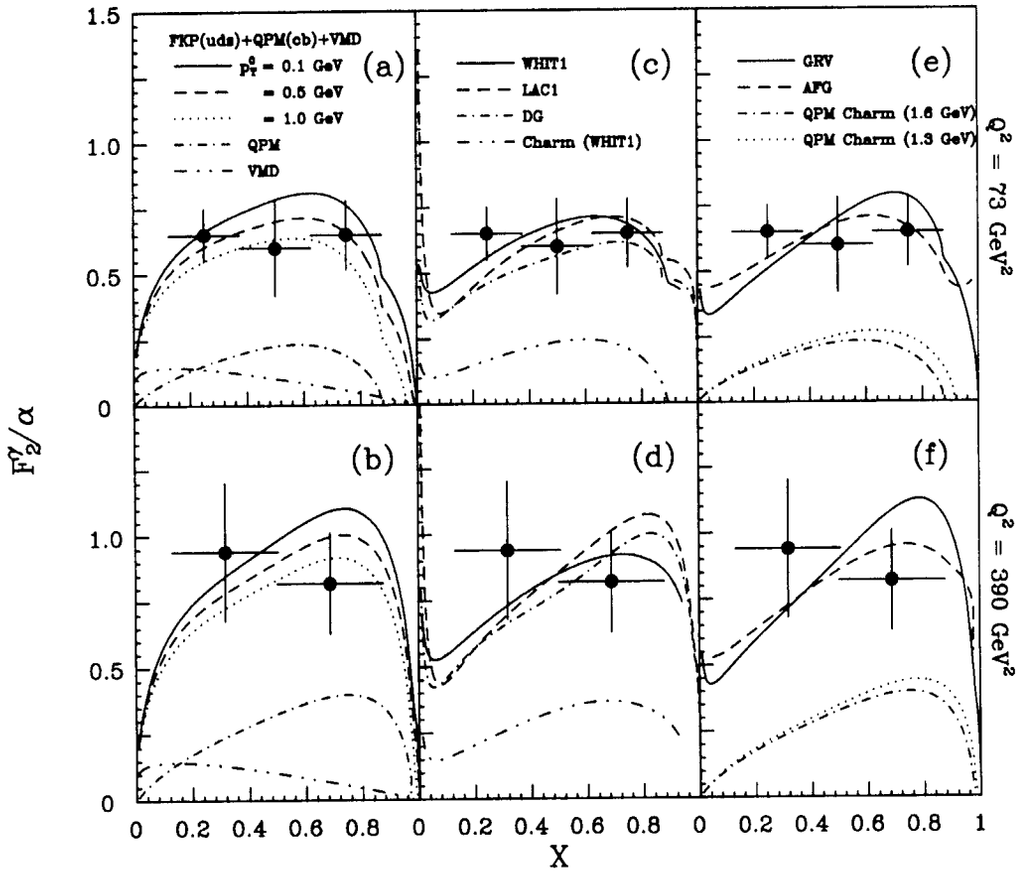

Figure 3

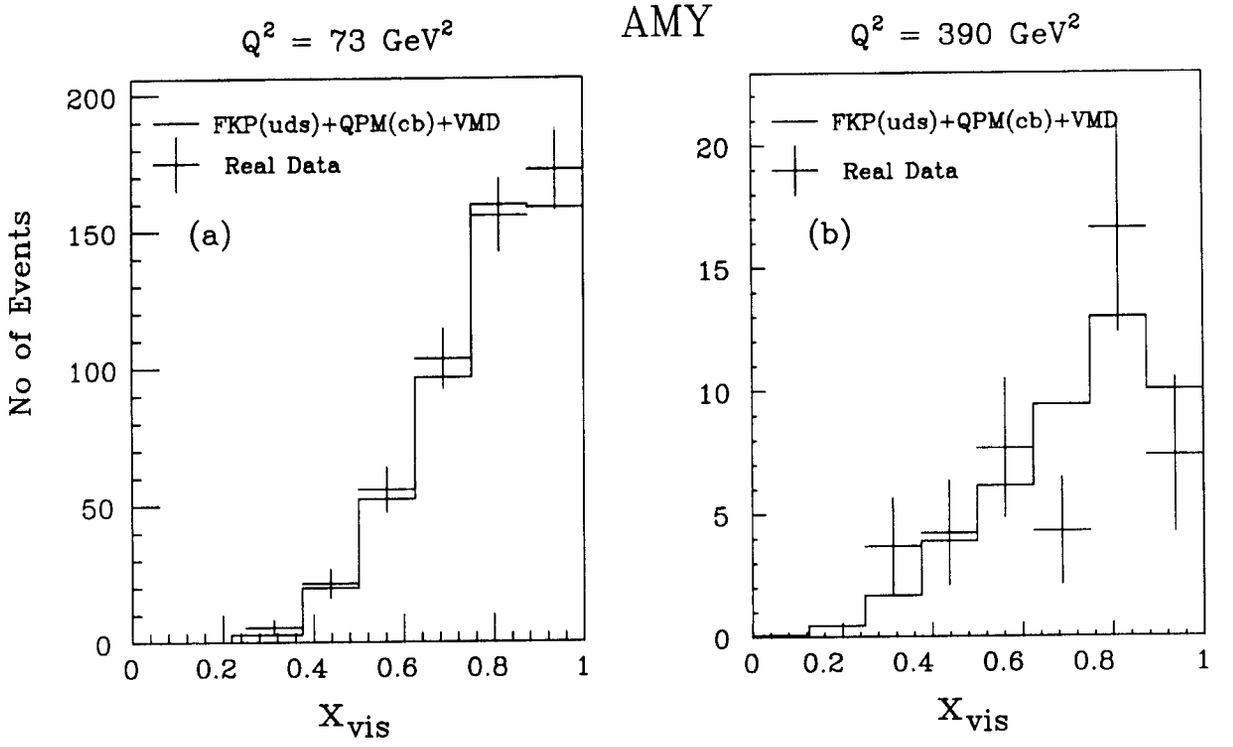

Figure 2

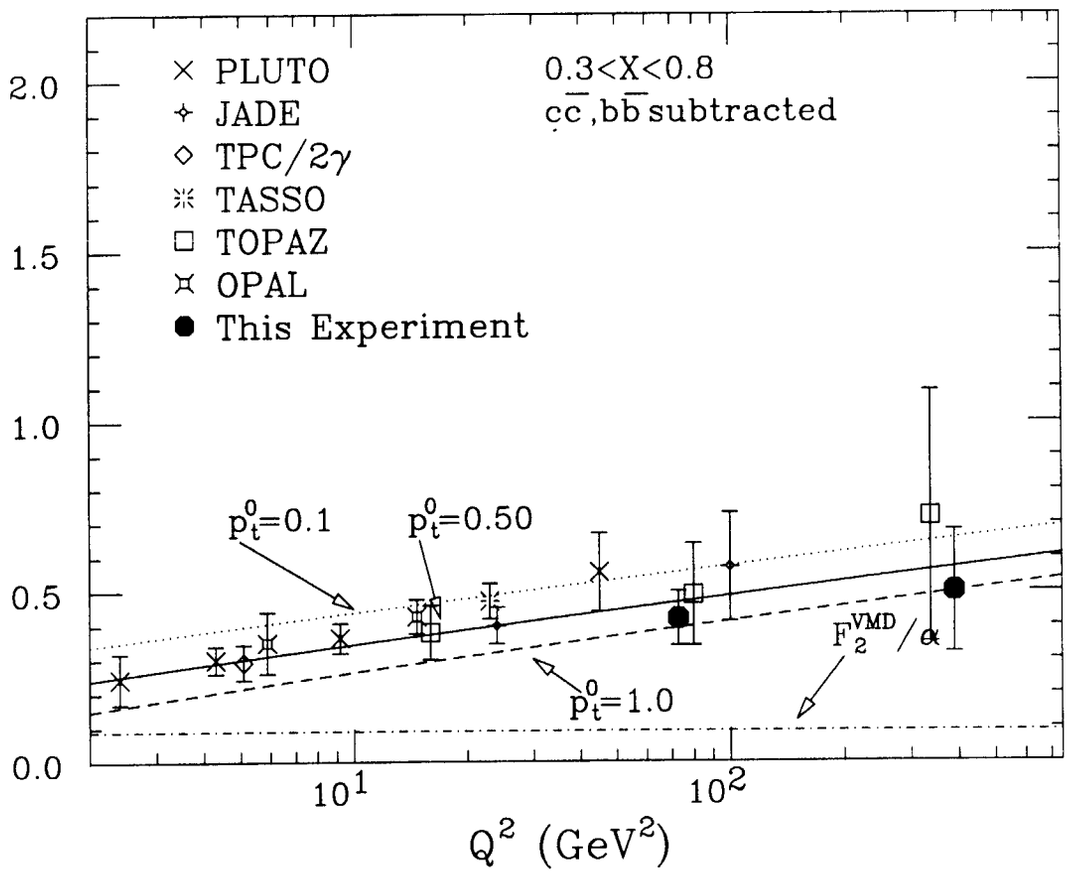
PLUTO
JADE
TPC/2γ
TASSO
TOPAZ
OPAL
This Experiment
0.3<X<0.8
cc̄, bb̄ subtracted
p_t^0=0.1
p_t^0=0.50
p_t^0=1.0
F_2^{VMD}/α
$<F_2^\gamma/\alpha>$
Q^2 (GeV^2)
2.0
1.5
1.0
0.5
0.0
10^1
10^2

Figure 4